A Large PEST-like Sequence Directs the Ubiquitination, Endocytosis, and Vacuolar Degradation of the Yeast a-Factor Receptor

Amy F. Roth, Daniel M. Sullivan, and Nicholas G. Davis

Departments of Surgery and Pharmacology, Wayne State University School of Medicine, Detroit, Michigan 48201

Abstract. The yeast **a**-factor receptor (encoded by *STE3*) is subject to two modes of endocytosis, a ligand-dependent endocytosis as well as a constitutive, ligand-independent mode. Both modes are associated with receptor ubiquitination (Roth, A.F., and N.G. Davis. 1996. *J. Cell Biol.* 134:661–674) and both depend on sequence elements within the receptor's regulatory, cytoplasmically disposed, COOH-terminal domain (CTD). Here, we concentrate on the Ste3p sequences required for constitutive endocytosis. Constitutive endocytosis is rapid. Receptor is synthesized, delivered to the cell surface, endocytosed, and then delivered to the vacuole where it is degraded, all with a $t_{1/2}$ of 15 min. Deletion analysis has defined a 36-residue-long sequence mapping near the COOH-terminal end of the Ste3p CTD that is the minimal sequence required for this rapid turnover. Deletions intruding into this interval block or severely slow the rate of endocytic turnover. Moreover, the same 36-residue sequence directs receptor ubiquitination. Mutants deleted for this sequence show undetectable levels of ubiquitination, and mutants having intermediate endocytosis defects show a correlated reduced level of ubiquitination. Not only necessary for ubiquitination and endocytosis, this sequence also is sufficient. When transplanted to a stable cell surface protein, the plasma membrane ATPase Pma1p, the 36-residue STE3 signal directs both ubiquitination of the PMA1-STE3 fusion protein as well as its endocytosis and consequent vacuolar degradation. Alanine scanning mutagenesis across the 36-residue-long interval highlights its overall complexity—no singular sequence motif or signal is found, instead required sequence elements distribute throughout the entire interval. The high proportion of acidic and hydroxylated amino acid residues in this interval suggests a similarity to PEST sequences—a broad class of sequences which have been shown to direct the ubiquitination and subsequent proteosomal degradation of short-lived nuclear and cytoplasmic proteins. A likely possibility, therefore, is that this sequence, responsible for both endocytosis and ubiquitination, may be first and foremost a ubiquitination signal. Finally, we present evidence suggesting that the true signal in the wild-type receptor extends beyond the 36-residue-long sequence defined as a minimal signal to include contiguous PEST-like sequences which extend another 21 residues to the COOH terminus of Ste3p. Together with sequences identified in two other yeast plasma membrane proteins, the STE3 sequence defines a new class of ubiquitination/endocytosis signal.

Key words: endocytosis • ubiquitin • *Saccharomyces cerevisiae* • pheromone • receptors

In mammalian cells, the events surrounding the initial cell surface capture of membrane proteins by receptor-mediated endocytosis are reasonably well understood (Mellman, 1996; Schmid, 1997). The process is selective with proteins destined for uptake being first sequestered into differentiated subdomains of the plasma membrane, i.e., clathrin-coated pits. Pits invaginate, pinching off as clathrin-coated membrane vesicles into the cytoplasm. Uptake selectivity is controlled through a specific binding interaction between the endocytosis signal, a peptidyl sequence localized to the cytoplasmically exposed domains of the membrane protein, and the adaptin complex, a component of the coated pit. Two varieties of such endocytosis signals have so far been identified. Y-based signals constitute a loosely conserved motif in which an aromatic residue, either tyrosine or phenylalanine plays a central role. L-based signals have a leucine–leucine dipeptide as the central recognizable feature. For both, the func-

Address all correspondence to N.G. Davis, Departments of Surgery and Pharmacology, Wayne State University School of Medicine, Elliman Building, room 1205, 421 E. Canfield, Detroit, MI 48201. Tel.: (313) 577-7807. Fax: (313) 577-7642. E-mail: ndavis@cmb.biosci.wayne.edu

tional signal is short and discrete, lying within a polypeptide sequence 5–10 residues long.

In the yeast *Saccharomyces cerevisiae*, much progress has been made in recent years in understanding endocytic processes. Genetic analyses have identified a large collection of cellular proteins that participate in this process, both at the initial plasma membrane uptake step as well as at the subsequent endosomal transport steps (Riezman et al., 1996). In spite of the wealth of genetic data, the molecular details of the initial cell surface uptake event remain surprisingly obscure. As for mammalian cells, the process is selective—only a subset of the plasma membrane proteins are subject to endocytosis, others, for instance, the plasma membrane ATPase, Pma1p, remain stably at the cell surface (Benito et al., 1991). Although clear homologues of the mammalian clathrin and adaptins have been identified, their direct involvement in this uptake remains uncertain. Mutants generated in the gene for the yeast clathrin heavy chain slow, yet do not block endocytic uptake (Payne et al., 1988; Tan et al., 1993). Much more profound effects are seen instead for mutants that disrupt the yeast cell's actin cytoskeleton. Mutants in actin, myosin, as well as in a variety of actin-associated proteins often lead to a near total block of the uptake process (Riezman et al., 1996).

Protein ubiquitination has also emerged as a regulator of initial endocytic uptake events both in yeast (Kolling and Hollenberg, 1994; Egner and Kuchler, 1996; Galan et al., 1996; Hicke and Riezman, 1996; Roth and Davis, 1996; Galan and Haguenauer-Tsapis, 1997; Kolling and Losko, 1997; Marchal et al., 1998) and in mammalian cells (Strous et al., 1996; Gowers et al., 1997). Ubiquitin, a small 76-residue protein, has long been known as a regulator of protein degradation in the cell cytoplasm. Covalent attachment of ubiquitin to selected lysyl residues targets the substrate protein for proteosomal degradation (Hochstrasser, 1996). The degradative turnover of plasma membrane proteins or of proteins that enter the cell via the endocytic route has generally been thought to involve a separate system, that being proteolysis by the proteases residing within the membrane-enclosed space of the lysosome. Nevertheless, for a number of years, a growing collection of mammalian cell surface proteins have found to have covalently attached ubiquitin (Ciechanover, 1994). Recently, these findings have been mirrored by similar findings in yeast where a number of different plasma membrane proteins have been found to be ubiquitinated. In yeast, studies designed to test the function of the ubiquitin modification draw a consistent picture, linking ubiquitination to endocytosis (Kolling and Hollenberg, 1994; Egner and Kuchler, 1996; Galan et al., 1996; Hicke and Riezman, 1996; Roth and Davis, 1996; Kolling and Losko, 1997; Galan and Haguenauer-Tsapis, 1997; Marchal et al., 1998). The general model that has emerged has ubiquitin attached to cytoplasmic portions of surface membrane proteins serving as a flag, signaling uptake. Strong support for this model comes from work on the α-factor receptor, one of the two pheromone receptors in yeast. In a first report, mutation of the presumptive lysyl ubiquitin acceptor site concomitantly abolished both ubiquitination and uptake (Hicke and Riezman, 1996) indicating a requirement for ubiquitination in endocytosis. In a second report, ubiquitin addition was found to provide a sufficient trigger for uptake: a translational in-frame fusion of a ubiquitin moiety to the cytoplasmic domain of an endocytosis-defective mutant α-factor receptor restored endocytic capacity (Terrell et al., 1998). Furthermore, the results of Terrell et al. (1998) also indicate a fundamental point of difference between ubiquitin's involvement in proteosomal degradation versus endocytosis. Whereas proteosomal recognition generally requires the elaboration of a multi-ubiquitin chain on the substrate protein (Hochstrasser, 1996), addition of a single ubiquitin moiety appears sufficient to specify α-factor receptor endocytosis (Terrell et al., 1998).

Both of the yeast pheromone receptors, the **a**- and α-factor receptors, have been well studied as paradigms for endocytosis. These two G protein–coupled receptors mediate the hormonal communication that precedes the sexual conjugation of the two yeast haploid mating types, the **a** cell with the α cell. Though sharing no primary sequence homology, both receptors couple to the same downstream signaling pathway (Bender and Sprague, 1986). Our analyses have focused mainly on the **a**-factor receptor encoded by the gene *STE3*. Ste3p has the canonical G protein–coupled receptor structure with seven transmembrane domains followed at the COOH terminus by, in the case of Ste3p, a relatively large 185-residue hydrophilic, cytoplasmically exposed, COOH-terminal tail domain (CTD).[1] The CTD is a regulatory domain and can be largely deleted without impairing the gross functioning of the receptor, i.e., ligand binding and G protein coupling (Boone et al., 1993). Though functional, receptors truncated for this CTD manifest an unregulated response to the **a**-factor ligand that is both exaggerated and prolonged. In addition, these mutant receptors are defective for the two uptake modes that have been demonstrated for this receptor—a constitutive or ligand-independent uptake mode, as well as a ligand-dependent endocytosis (Davis et al., 1993; Tan et al., 1996). Both modes involve ubiquitination (Roth and Davis, 1996) and both deliver surface receptor to the vacuole for degradation by the resident proteases (the vacuole is the yeast equivalent organelle to the mammalian lysosome). Though both receptors are subject to the two uptake modes, for the **a**-factor receptor, constitutive endocytosis is by far the more prominent, transporting unliganded receptor from surface to vacuole for degradation with a $t_{1/2}$ of 15 min. Furthermore, at least for Ste3p, the two uptake modes are mechanistically distinct. The two are controlled by distinct signals mapping to distinct portions of the receptor CTD (Davis et al., 1993; Tan et al., 1996). Second, the two are distinguished by the participating cellular functions required for each: mutants in the ankyrin-repeat protein Akr1p block constitutive endocytosis of the **a**-factor receptor, yet have no effect on ligand-dependent uptake (Givans and Sprague, 1997). In spite of these differences, much of the mechanism may also be shared. Receptor ubiquitination and vacuole-directed transport are common to both and both are blocked by mutants in the actin-associated function *SLA2/END4* (Roth and Davis, 1996), suggesting a requirement of the actin cytoskeleton for both uptake modes.

1. *Abbreviations used in this paper*: CTD, cytoplasmically disposed, COOH-terminal domain; ORF, open reading frame.

In the present work we characterize the sequences within the **a**-factor receptor CTD required for its rapid ligand-independent endocytosis, i.e., the constitutive endocytosis signal. Although an expanding collection of plasma membrane proteins have now been shown to undergo endocytosis in yeast, the signals that direct uptake have been studied in just a few cases. For the two pheromone receptors, sequences required for ligand-dependent endocytosis have been characterized. The α-factor receptor CTD sequence DAKSS has been shown to be required for ligand-dependent uptake of a mutant receptor deleted for the COOH-terminal two-thirds of its 128-residue-long CTD (Rohrer et al., 1993). The central lysine in this sequence appears to serve as the acceptor site for ubiquitin attachment (Hicke and Riezman, 1996). For the **a**-factor receptor, the sequence NPFXD is required for ligand-dependent endocytosis (Tan et al., 1996).

The work that follows characterizes the sequences within the **a**-factor receptor, which direct its rapid, constitutive endocytosis. We find that a 36-residue-long sequence directs both uptake as well as the associated ubiquitination of the receptor. No obvious resemblance to either the mammalian L- or Y-based endocytosis signals or to the two signals characterized for the ligand-dependent uptake of the two yeast pheromone receptors is apparent. Instead, rich in both acidic and hydroxylated amino acids, the Ste3p signal bears a resemblance to the PEST sequences that direct ubiquitination and proteosomal turnover of short-lived cytoplasmic and nuclear proteins. Recent reports on two other yeast plasma membrane proteins, the **a**-factor export protein Ste6p and the uracil permease Fur4p, identify similar PEST-like sequences as participating in their constitutive endocytosis (Kolling and Losko, 1997; Marchal et al., 1998). Together these three sequences likely represent a new class of endocytosis signal—signals where the primary function may be to direct the addition of an initiating ubiquitin.

Materials and Methods

Plasmids

Three *URA3*/2μ plasmids were constructed for *CUP1*-driven overexpression of wild-type or myc-tagged ubiquitin (Ellison and Hochstrasser, 1991). pND186 (*CUP1*-ubiquitin), pND747 (*CUP1*-myc-ubiquitin), and pND187 (*CUP1* promoter only) were constructed through the replacement of the ClaI–BamHI interval of YEp24 with the *CUP1*-ubiquitin–containing ClaI–BamHI fragment from the corresponding *URA3/CEN/ARS* plasmids pND164, pND165, and pND167, respectively (Roth and Davis, 1996).

The other plasmids constructed and used in this work divide into series of equivalent constructs carrying either wild-type *STE3* or *STE3* mutant versions. The strategy used in the construction of each series is reported in the following three sections.

Construction of In-Frame Deletions

For constructing in-frame deletions within the Ste3p CTD, the general strategy involved introduction of XhoI restriction sites by oligonucleotide-directed mutagenesis at various positions within the *STE3* CTD-encoding sequences. Restriction and then ligation of upstream to downstream sites deletes the interval in between. Each XhoI site mutation replaced two adjacent *STE3* codons with the sequence CTCGAG. Each replacement encoded the dipeptide leucine-glutamate and ligation of any two sites results in in-frame translation across the deletion.

Eight XhoI site mutations were constructed, at each of the following dipeptide codons: $Leu_{398}Lys_{399}$, $Phe_{413}Asp_{414}$, $Ser_{423}Lys_{424}$, $Leu_{433}His_{434}$, $Phe_{441}Glu_{442}$, $Leu_{446}Cys_{447}$, $Pro_{450}Ala_{451}$, and $Ser_{458}Ser_{459}$. In addition, a SalI site compatible with the XhoI sites was introduced at the $Leu_{320}Leu_{321}$ dicodon changing it to $Val_{320}Asp_{321}$.

Oligonucleotide-directed mutagenesis was by the method of Kunkel et al. (1987). The ssDNA template was derived from pSL1839, a 5.5-kb BamHI–SalI fragment from the original *STE3* genomic library isolate (Hagen et al., 1986) carried on pRS306 (Sikorski and Hieter, 1989). Mutant plasmids for each restriction site were subjected to DNA sequencing in the vicinity of the site to confirm the fidelity of the mutagenesis.

Two additional SalI restriction sites, compatible with the XhoI site reading frames, were also used: the natural SalI site at *STE3* codons 364 and 365, as well as a SalI site introduced via linker ligation to the PstI site located at *STE3* codons 466–468 (see pSL1922 in Davis et al., 1993). This linker-derived SalI site was used in combination with the different XhoI site mutants to construct the series of "COOH-terminally"-truncated *STE3* mutants. In fact, these truly are in-frame deletions, as they all retain the natural COOH-terminal STE3 dipeptide $Gly_{469}Pro_{470}$.

Assessment of receptor ubiquitination levels required that each of the receptor mutants be overexpressed from the *GAL1* promoter. The plasmid pSL552 (Bender and Sprague, 1986) has a *GAL1*-controlled wild-type *STE3* gene carried on the yeast *URA3/CEN/ARS* plasmid YCp50 (Rose et al., 1987). In-frame *STE3* deletions constructed above in the pSL1839 plasmid context, were introduced into pSL552 via replacement of 380-bp SalI–SacI restriction fragment covering the COOH-terminal coding portion of *STE3*, with the equivalent fragment containing the desired deletion mutation.

Construction of Triple Alanine Substitution Mutations

The 12 triple alanine mutations created within the 414–449 interval of *STE3* (see Fig. 8) also were constructed via oligonucleotide-directed mutagenesis (Kunkel et al., 1987). For each, three adjacent *STE3* codons are replaced by the sequence GCTGCAGCC, encoding three consecutive alanines. This substitution also introduces a PstI site, allowing identification of the mutant clone by restriction analysis. The ssDNA template for mutagenesis was from pND210, the *Δ450–468* mutant version of pSL1839. Fidelity of mutagenesis was confirmed for each via DNA sequencing in the vicinity of mutation site.

Two of the triple alanine mutations were also constructed within the context of wild-type (i.e., full-length) *STE3*. Reconstruction of *STE3* with either the 417–419 or 426–428 triple alanine mutations (see Fig. 9) used the HindIII site at codons 433, 434, allowing the wild-type COOH-terminal *STE3* sequences to be restored to the *STE3Δ450–468* versions of these mutations.

Construction of PMA1-STE3 Fusions

The plasmid pXZ28 (Harris et al., 1994) has a *GAL1*-driven HA epitope–tagged *PMA1* gene carried on a yeast *URA3/CEN/ARS* plasmid. The single HA epitope tag inserted near the NH_2-terminal coding sequences, following the second codon of *PMA1* does not affect *PMA1* function. The 750-bp EcoRI–XhoI pXZ28 *GAL1* promoter fragment plus the 3.6-kb XhoI–PstI *HA-PMA1*–containing pXZ28 fragment were inserted into the polylinker of the yeast *LEU2/CEN/ARS* vector pRS315 (Sikorski and Hieter, 1989) between EcoRI and SacI to give pND533. This required modification of the PstI end of the 3.6-kb fragment by addition of a SacI linker. The unique XhoI site of pND533, at the fusion boundary between *GAL1* and *PMA1* sequences was destroyed via end-filling and re-ligation to give pND542. To create pND563, the immediate progenitor of *PMA1-STE3* fusion protein plasmids, a new XhoI site was introduced into *PMA1* by oligonucleotide-directed mutagenesis at COOH-terminal position two residues from the end of the coding sequences (the XhoI site substitutes for the codons $Lys_{916}Glu_{917}$). The *PMA1* XhoI site is designed to accommodate in-frame fusions with the *STE3* XhoI sites. For most of these fusions the XhoI site at *STE3* codons 398, 399 was used (see above) with the contributed *STE3* sequences extending from codon 400 to different COOH-terminal endpoints. For instance, to construct the *PMA1-STE3(400–440)* fusion protein, the 398, 399 XhoI site was introduced via oligonucleotide-directed mutagenesis into the *STE3Δ441–468* deletion mutant context. From this plasmid, a 250-bp XhoI–SacI fragment could be excised (the SacI site is located 3′ of the *STE3* open reading frame [ORF]) and used to replace the XhoI–SacI fragment from the GAL1-HA-PMA1 plasmid pND563.

Strains

Genotype and source for some of the yeast strains used in this work are reported in Table I. The two new strains listed, NDY343 and NDY344, isogenic *ste3Δ::LEU2* versions of the strains NDY334 and NDY335 (Roth and Davis, 1996), were constructed via the two-step gene replacement strategy (Boeke et al., 1987) as described previously (Roth and Davis, 1996), wherein a *ste3Δ::LEU2* allele was used to replace *STE3*. The *ste3Δ::LEU2* allele, carried on the integrating plasmid pSL2165, a pSL1839 derivative (see "Plasmids"), in which the entire *STE3* ORF is replaced by the 2.85-kb BglII *LEU2* fragment. The *ste3* deletion extends from a point 417 bp upstream of the *STE3* ORF to a point 111 bp downstream. pSL2165 was uniquely restricted at a SfiI site located upstream of *STE3* to direct chromosome insertion.

In addition to the strains reported in Table I, numerous other strains were constructed and used in this work. The turnover of each Ste3p mutant was measured in strains in which the mutant *STE3* allele replaces the *ste3Δ::LEU2* allele of NDY343. This strain construction used the two-step gene replacement strategy (Boeke et al., 1987) as previously described (Roth and Davis, 1996). For each, the transplacing allele, derivatives of the integrating plasmid pSL1839 with the mutant *STE3* in place of wild-type *STE3*, were restricted with HpaI to direct chromosomal insertion. This eliminated one potential source of experimental variability—differences in receptor expression levels resulting from clonal fluctuations in plasmid copy number.

Antibodies

Rabbit antisera was raised against the STE3 CTD, as part of one of two bacterial fusion proteins, TrpE-STE3 (Clark et al., 1988) or MalE-STE3. All Ste3p-specific antisera were affinity purified to the MalE-STE3 antigen coupled to CNBr-activated Sepharose 4B (Sigma Chemical Co., St. Louis, MO). The HA.11 mAb (Berkeley Antibody Co., Berkeley, CA) was used for detection of HA epitope–tagged PMA1-STE3 fusions. The myc mAb (Oncogene Research, Uniondale, NY) was used for detection of the myc 9E10 epitope–tagged ubiquitin (Ellison and Hochstrasser, 1991). Pgk1p-specific antiserum was generously provided by T. Stevens (University of Oregon, Eugene, OR).

Cell Labeling, Extract Preparation, and Immune Precipitation

Pulse-chase analysis (Roth and Davis, 1996) entailed in vivo labeling of yeast cultures via a 10-min pulse of [^{35}S]methionine, which was followed by addition of the non-radioactive chase: methionine added to a concentration of 750 μg/ml, cysteine to 150 μg/ml, and yeast extract to 0.2%. At various times after chase addition, culture aliquots were removed and extracts were prepared by the glass bead method described previously (Roth and Davis, 1996). Wild-type or mutant receptors were then isolated via two iterative rounds of immunoprecipitation (Roth and Davis, 1996). Each round used different affinity-purified anti-Ste3p antibodies derived from the polyclonal antisera of different rabbits. Immunoprecipitated samples were subjected to SDS-PAGE, and then both to autoradiography and to Storm PhosphorImaging (Molecular Dynamics, Inc., Sunnyvale, CA) for the quantitative analysis.

For immunoprecipitation of the HA-tagged PMA1-STE3 fusion proteins, 20 μl of extract corresponding to 50×10^6 cells, prepared as described (Davis et al., 1993), was subjected to a single round of immunoprecipitation (Roth and Davis, 1996) using 30 μl of a slurry of the HA.11 mAb conjugated to agarose beads (Berkeley Antibody Co.). Incubation with the mAb in this case was for 16 h at 4°C.

Table I. Yeast Strains

Strain	Genotype	Reference or source*
SY1574	*MAT*α *STE3 ura3 leu2 ade2-1^{oc} ade1 his6 trp1^{am}*	Davis et al., 1993; A
SY2601	*MAT*α *STE3 pep4Δ*	Roth and Davis, 1996; A
SY2602	*MAT*α *ste3Δ::LEU2 pep4Δ*	Roth and Davis, 1996; A
RH268-1C	*MAT***a** *end4-1 ura3 leu2 his4 bar1-1*	Raths et al., 1993; B
NDY334	*MAT*α *END4*	Roth and Davis, 1996; B
NDY335	*MAT*α *end4-1*	Roth and Davis, 1996; B
NDY343	*MAT*α *ste3Δ::LEU2 END4*	This work; B
NDY344	*MAT*α *ste3Δ::LEU2 end4-1*	This work; B

*Strains designated *A* are isogenic to SY1574. Strains designated *B* are isogenic to RH268-1C.

Susceptibility to External Proteases

To assess the susceptibility of newly synthesized receptor to digestion by extracellular proteases, cells were first subjected to in vivo labeling via the pulse-chase protocol described above. At various times after chase addition, culture aliquots were removed and intact cells were treated with Pronase (Calbiochem-Novabiochem Corp., La Jolla, CA) and protein extracts were prepared (Davis et al., 1993). Immunoprecipitation and further analysis was as described above.

Protein Extract Preparation, Western Analysis, and Phosphatase Treatment

For Western analysis, the relevant *STE3* mutant or PMA1-STE3 fusion protein was expressed from the *GAL1* promoter. For these experiments, overnight log-phase cultures in rich YP medium containing 2% raffinose were inoculated from minimal plates on which plasmid retention was selected. Induction of the *GAL1* promoter involved the addition of galactose to 2%. The duration of the galactose induction was as indicated for each figure and was terminated when synthesis repression was desired with the addition of glucose to 3%. Protein extract preparation, SDS-PAGE, and Western analysis were as described previously (Roth and Davis, 1993).

Treatment of protein extracts with potato acid phosphatase (Boehringer Mannheim Corp., Indianapolis, IN) at a final concentration of 0.06 U/ml was as described previously (Roth and Davis, 1996).

Quantitation of the Proportion of Receptor Protein with Attached Ubiquitin

Quantitating the proportion of receptor proteins with attached ubiquitin was by Western analysis of phosphatase-treated protein extracts for the various *STE3* mutants. Quantitative AMBIS densitometry of films (AMBIS Systems, Inc., San Diego, CA) resulting from ECL development of the Western blot (Amersham Corp., Arlington Heights, IL) was used to estimate the relative amount of the receptor protein present in the two ubiquitin-modified electrophoretic positions (the presumptive mono- and di-ubiquitinated forms; Roth and Davis, 1996), and at the unmodified position. Many aspects of this analysis rely on techniques wherein the measured output is produced non-linearly. To circumvent this potential source of error, we have compared signals only of similar intensity levels. This was achieved by applying the Western analysis to a dilution series for each sample. For instance, with phosphatase-treated extracts derived from wild-type Ste3p, the intensity level of the signal associated with the mono-ubiquitinated band was found to be intermediate between the level of the unmodified receptor band present from the 1:5 and 1:25 dilutions of the same extract. Quantitative densitometry of the band signals from the same compared samples led to the determination that 10% of the wild-type receptor was present in the mono-ubiquitinated species band. As 10% was also present in the di-ubiquitinated band, the summed estimate of 20% was reported in Fig. 3 as proportion of receptor ubiquitinated.

Results

Identification of a Receptor Subdomain That Directs Rapid Constitutive Endocytosis

Our previous work showed that the rapid constitutive endocytosis of Ste3p requires sequence elements within the COOH-terminal 72–amino acid residues of the receptor (Davis et al., 1993). To better delineate this requirement we have constructed a series of in-frame deletion mutants within the receptor's dispensable CTD. First we have first investigated if CTD sequences in addition to the 72-residue COOH-terminal segment are required for rapid constitutive endocytosis. The 187-residue-long Ste3p CTD extends from Asp_{284} (the first charged residue after the

seventh transmembrane segment) to a COOH-terminal Pro_{470}. Three large deletion mutants, deleting residues 320–363 (*STE3Δ320–363*), residues 365–414 (*STE3Δ365–414*), and the COOH-terminal residues 413–468 (*STE3Δ413–468*) were used. As a first assessment of endocytosis, the rate of degradative turnover of each of the different receptor mutants was determined (Fig. 1 *A*). While wild-type Ste3p turns over rapidly with a $t_{1/2}$ estimated to be ~15 min, the *Δ413–468* mutant receptor is completely stable, indicating that the COOH-terminal 58 residues are required for this ligand-independent receptor turnover. Like wild-type, both the *Δ365–414* and *Δ320–363* receptors show rapid turnover consistent with endocytosis that is largely unimpaired. Thus, of the *STE3* CTD sequences, the COOH-terminal 58 residues play the primary role in specifying rapid turnover. We have therefore concentrated our analyses on this interval.

The turnover defect of Ste3Δ365–468p, a mutant missing its COOH-terminal 105 residues, is a consequence of blocked endocytic transport from surface to vacuole (Davis et al., 1993). With endocytosis blocked the receptor accumulates at the cell surface. If the turnover defect of the *Δ413–468* mutant receptor also results from impaired endocytosis, then this receptor should also accumulate at the cell surface. To assess surface localization of the *Δ413–468* receptor, we have used protease susceptibility as a probe, testing the accessibility of the receptor within whole cells to digestion by added, external protease. This assay distinguishes surface-localized receptor (susceptible to external proteases), from receptor that localizes to compartments inside the cell (resistant to external proteases) (Davis et al., 1993). As for Fig. 1 *A*, cells were subjected to pulse-chase analysis. At various times after the initiation of the non-radioactive chase, aliquots of the labeled, intact cells were subjected to protease treatment (Fig. 1 *B*). Digestion of surface-localized receptor is evident both in terms of loss of receptor protein and by the production of a protease digestion product corresponding to the protected, intracellular CTD plus final transmembrane domain (Davis et al., 1993; the antibody used for the immunoprecipitation is *STE3* CTD specific). Wild-type Ste3p in such a regimen is only transiently susceptible to the added proteases, reflective of its short surface residency time (Davis et al., 1993). Here, we find that the *Δ413–468* mutant receptor remains susceptible to the proteases even 90 min after synthesis (Fig. 1 *B*). Quantitation via PhosphorImaging indicates that 75% of *Δ413–468* receptor protein is susceptible to protease 45 min after synthesis and 60% remains susceptible at the 90-min time point. Cell integrity is maintained throughout the digestion protocol as evidenced by the complete protection from digestion of a cytoplasmic marker protein, phospho-glycerol kinase (Pgk1p; Fig. 1 *B*, *bottom panel*). We conclude from its prolonged surface residency time that turnover defect found for Ste3Δ413–468p does indeed reflect impaired endocytosis.

Deletional Analysis of the Sequences Required for Rapid Endocytosis and Turnover

To identify the sequence element(s) that direct the constitutive endocytosis of Ste3p we have constructed a finer series of deletions within the 413–468 interval. First we tested the effects of three deletions extending progressively in from the receptor COOH terminus. The in vivo rate of turnover was assessed for wild-type Ste3p and for each mutant receptor via a pulse-chase regimen similar to that described for Fig. 1 *A*. Immunoprecipitated receptors were subjected to SDS-PAGE (Fig. 2 *A*) and then to PhosphorImaging analysis to quantitate their rate of loss to degradation (Fig. 2 *B*). As seen previously (Fig. 1 *A*), turnover is rapid for wild-type Ste3p and wholly blocked for Ste3Δ413–468p. The two intermediate deletion mutants, *Δ450–468* and *Δ441–450* show intermediate rates of turnover. Quantitation of the receptor-associated radioactivity at each time-point is shown in Fig. 2 *B*. Most of the data points for each receptor conform to a linear plot, allowing the calculation of turnover half-life for each mutant (Fig. 2 *B*). For wild-type Ste3p, a $t_{1/2}$ of 16 min is calculated. For Ste3Δ450–468p, turnover remains rapid, though somewhat less so than wild-type: a $t_{1/2}$ of 21 min is calculated. With the progressive extension of these deletions, a progressive impairment is evident. A $t_{1/2}$ of 65 min is calculated for the *Δ441–468* receptor and the turnover block appears to be complete for the *Δ413–468* receptor.

For two of the receptors, namely wild-type and *Δ450–468*, the 90-min time-points fail to conform to the line defined by the other time-points (Fig. 2 *B*). This is seen consistently and indicates that a minority of these receptors,

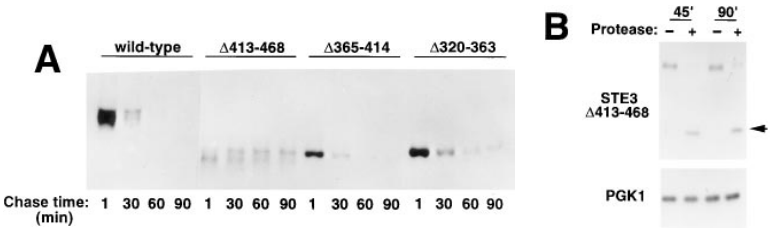

Figure 1. Analysis of the CTD sequences that contribute to the rapid, constitutive endocytosis of Ste3p. Yeast strains were subjected to [^{35}S]methionine pulse-chase analysis as described in the Materials and Methods. (*A*) Contribution of CTD sequences to Ste3p constitutive turnover. Cells from four isogenic strains were tested: NDY334, a wild-type *MAT*α strain, as well as three strains differing only in their *STE3* allele, these being either *STE3Δ413-468*, *STE3Δ365-414*, or *STE3Δ320-363*. Receptor immunoprecipitated from labeled extracts prepared at the indicated chase times was subjected to SDS-PAGE, and then visualized by autoradiography. (*B*) Surface-localization assessment for the turnover defective deletion mutant receptor Ste3Δ413-468p. The *STE3Δ413-468* strain of part A was subjected to pulse-chase analysis as above. At the two indicated chase times, 45 min and 90 min after addition of the excess non-radioactive methionine and cysteine, culture aliquots were removed and whole, energy-poisoned cells were treated with proteases (+), or mock-treated (−), as described in the Materials and Methods. Protein extracts prepared from each sample were subjected to immunoprecipitation with either Ste3p-specific (*top panel*) or Pgk1p-specific (*bottom panel*) antibodies, followed by SDS-PAGE and autoradiography. The arrow at right indicates the position of the protected, CTD digestion product for Ste3Δ413-468p.

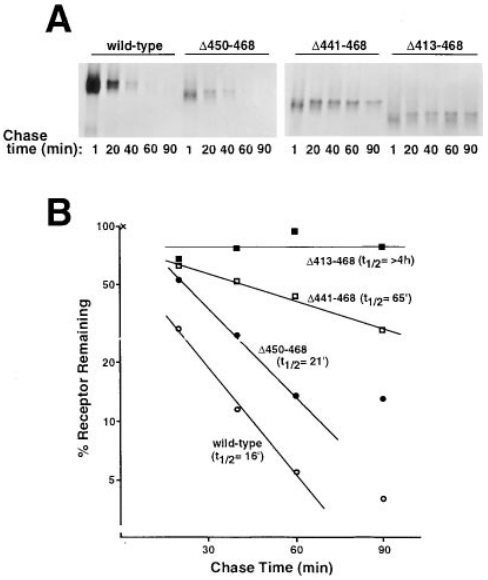

Figure 2. Turnover rate of different COOH-terminally truncated **a**-factor receptors. The wild-type *MAT*α strain NDY334 and three isogenic strains with different transplaced *STE3* alleles: *STE3Δ450-468*, *STE3Δ441-468*, or *STE3Δ413-468* were subjected to pulse-chase analysis and otherwise treated as described for Fig. 1 *A*. (*A*) Effect of COOH-terminal deletions on receptor turnover. Autoradiography of the SDS-PAGE of the immunoprecipitated receptor mutants. (*B*) Determination of the turnover $t_{1/2}$ for the receptor mutants. Phosphorimager analysis was applied to the polyacrylamide gel of *A* (Materials and Methods). For each strain, the radioactivity associated with receptor bands at the initial 1-min chase time-point was normalized to 100%. A semi-log plot of the radioactivity remaining associated with the receptor bands at each of the subsequent chase time-points is shown. For each strain, a turnover $t_{1/2}$ was calculated (indicated for each as $t_{1/2}$) from the slope of the line drawn through the linear portion of each data set.

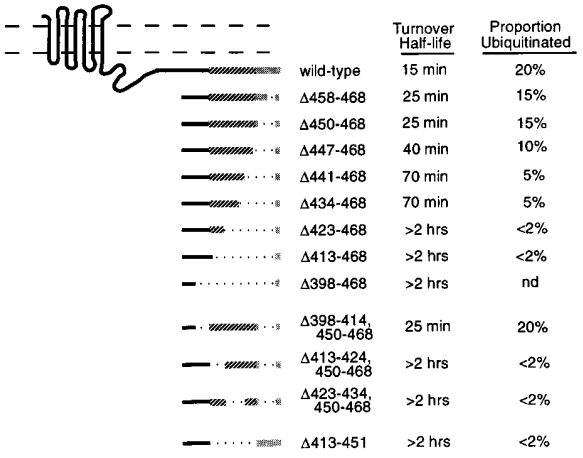

	Turnover Half-life	Proportion Ubiquitinated
wild-type	15 min	20%
Δ458-468	25 min	15%
Δ450-468	25 min	15%
Δ447-468	40 min	10%
Δ441-468	70 min	5%
Δ434-468	70 min	5%
Δ423-468	>2 hrs	<2%
Δ413-468	>2 hrs	<2%
Δ398-468	>2 hrs	nd
Δ398-414, 450-468	25 min	20%
Δ413-424, 450-468	>2 hrs	<2%
Δ423-434, 450-468	>2 hrs	<2%
Δ413-451	>2 hrs	<2%

Figure 3. Summary of turnover rates and the proportion of receptor proteins that are ubiquitinated for a collection of *STE3* deletion mutants constructed within the COOH-terminal 73 amino acid residues of Ste3p. Shown in the upper left is the hypothesized transmembrane structure for Ste3p. The region corresponding to the COOH-terminal 57 residues of the Ste3p CTD is highlighted, the 414–451 interval indicated with a striped box and the 451–470 interval by a stippled box. Shown below are sequences deleted (*dotted line*) for each of the different in-frame *STE3* deletion mutants tested. To the right, the exact amino acids residues removed for each mutant are indicated. The two columns at the right summarize the results of the two different experiments that were performed for each receptor, these being: (*1*) measurement of the turnover $t_{1/2}$, and (*2*) measurement of the proportion of the receptors found to be ubiquitinated. Measurement of turnover rate used a collection of strains isogenic to NDY334, except for the indicated *STE3* mutant alleles. As described in Fig. 2, each strain was subjected to pulse-chase labeling, immunoprecipitation, SDS-PAGE, phosphorimaging, and turnover $t_{1/2}$ calculation. In terms of experimental variability, half-lives calculated from different experiments were within 20% of the reported value for each mutant. Different conditions were required to assess receptor ubiquitination levels. Cells of the *MAT*α *ste3Δ pep4Δ* strain SY2602 transformed by either pSL552 (*GAL1-STE3*) or by the identical plasmid with the indicated *STE3* deletion allele in place of the wild-type *STE3* were grown and processed as described for Fig. 4 *A*. Quantitation of the proportion of receptor antigen localizing to the putative mono- and di-ubiquitinated receptor species was as described in the Materials and Methods. The values reported in the far right-hand column represent the combined sum of the receptor antigen present in the mono- and di-ubiquitinated forms. For the *Δ398-468* receptor mutant the proportion of receptor ubiquitinated was not determined (*nd*).

3% for wild-type and 13% for Ste3Δ450–468p, do not participate in the normal endocytic turnover mechanism. Hypothetically, these could be receptors in the process of undergoing recycling or receptors that are trapped to a locale that prohibits their endocytosis.

Fig. 3 summarizes the results from a total of eight COOH-terminal deletion mutants. Again, it is apparent that endocytic function is lost gradually with progressive removal of sequences from the COOH-terminal end. A small, but significant slowing of the turnover rate is apparent with removal of the COOH-terminal 12 amino acids (Fig. 3; $t_{1/2}$ of 25 min for *Δ458–468* vs. 15 min for wild-type). A second transition is broached with the *Δ447–468* deletion; the $t_{1/2}$ for turnover slows from 25 to 40 min. Further impairment is seen when the deletion is extended to residue 441, with the $t_{1/2}$ for *Δ441–468* being 70 min. Finally, with the deletion extended to residue 423, endocytosis appears to be wholly blocked. This gradual loss of function for deletions extending over the COOH-terminal 48 amino acids indicates the "signal" for constitutive endocytosis may be large and complex, potentially composed of redundant functional elements.

To delimit the upstream boundary of this endocytosis signal, small internal deletions were introduced into the *Δ450–468* mutant receptor. The *Δ450–468* deletion removes the COOH-terminal 20 amino acid residues and was used as the context for these other small deletions to eliminate the potential contribution of redundant elements within the 450–470 interval. The experiment of Fig. 1 indicated that a large portion of the receptor CTD (the 320–414 interval) is not required for rapid endocytic turnover. Again here within the *Δ450–468* context, introduction of a second deletion of residues 398–414 caused no additional defect; the $t_{1/2}$ for turnover of the double deletion mutant *Δ398–414*, *450–468* was unchanged from that of the parental *Δ450–468* construct (Fig. 3). However, introduction of either the *Δ413–424* or the *Δ423–434* dele-

tions into the *Δ450–468* receptor wholly blocked turnover. This indicates that sequences required for rapid endocytosis extend to the NH_2-terminal side of residue 423, potentially as far as residue 413. Thus, the 36-residue-long 414–449 sequence interval appears to be the most critical for directing rapid endocytosis. Consistent with this, deletion of just these amino acids (*STE3Δ413–451*) abolishes turnover (Fig. 3). However, the COOH-terminal 20 residues also may contribute to turnover: both the *Δ450–468* and *Δ458–468* deletions have small, but significant effects on the turnover rate (Figs. 2 and 3). Support for the participation of the COOH-terminal 20 residues in endocytosis is offered below (see Fig. 9) with experiments indicating a functional redundancy between sequence elements in the 414–449 interval and those in the 450–470 interval.

Sequences That Direct Receptor Endocytosis Also Direct Receptor Ubiquitination

We next tested if the *STE3* mutants defective for constitutive endocytosis are also defective for the associated constitutive ubiquitination. Receptor ubiquitination levels of the various *STE3* mutants were assessed via Western analysis: ubiquitinated receptor species manifest an 8-kD shift with each added ubiquitin moiety. Detection of the ubiquitinated forms is improved with the use of several key experimental conditions, including receptor overproduction (~10-fold) from the *GAL1* promoter. This enhances detection of the ubiquitinated forms, yet neither alters receptor turnover rate nor the proportion of the receptor subject to ubiquitination (data not shown). Secondly, to avoid loss of the ubiquitinated forms to vacuolar degradation, *pep4Δ* mutants deficient in vacuolar protease activity were used. Finally, treatment of protein extracts with phosphatase before electrophoresis eliminates the substantial heterogeneity in gel mobility because of the heterogenous phosphorylation of Ste3p (Fig. 7; also Roth and Davis, 1996).

In Fig. 4 *A*, the ubiquitination of three receptor mutants is compared with wild-type. For wild-type, the majority species (~80%) has no attached ubiquitin (Roth and Davis, 1996). The remaining 20% distributes almost equally between two, more slowly-migrating, ubiquitinated forms (indicated in Fig. 4 *A*, *arrows* at *left*), the mono- and di-ubiquitinated receptor species (Roth and Davis, 1996). Mutants that block endocytosis, namely *Δ413–468* and *Δ413–451* (Fig. 3), also blocked receptor ubiquitination (Fig. 4 *A*). Furthermore, the *Δ450–468* mutant receptor that showed diminished turnover (Fig. 2) also shows diminished ubiquitination (Fig. 4 *A*). Quantitation of these results along with similar analyses applied to the other mutant receptors is reported in Fig. 3. Comparison of the turnover half-life with ubiquitination levels shows a consistent correlation between the two—further compelling evidence for a functional connection linking ubiquitination and endocytosis.

Previously, we have shown that in *end4-1* cells, constitutive Ste3p endocytosis is blocked and the receptor is consequently trapped at the cell surface in a ubiquitinated state (Roth and Davis, 1996). Here, we again make use of the *end4* mutant strain background to eliminate endocytosis as a possible contributing cause to the differences seen

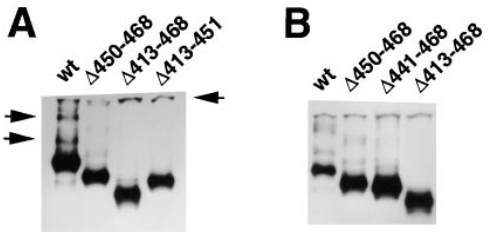

Figure 4. Assessment of receptor ubiquitination levels for *STE3* deletion mutants. (*A*) Phosphatase-treated *STE3* deletion mutant receptors expressed from the *GAL1* promoter in a *pep4Δ* cells. 2 h of growth in galactose medium was used to induce receptor expression in *MATα ste3Δ pep4Δ* cells (strain SY2602) transformed by a *CEN/ARS* plasmid with wild-type (*wt*) *STE3* under the control of the *GAL1* promoter (pSL552), or by the equivalent plasmid having one of three different *STE3* mutant alleles, either *STE3Δ450-468*, *STE3Δ413-468*, or *STE3Δ413-451*. Extracts were prepared and subjected to phosphatase digestion, SDS-PAGE, and finally anti-Ste3p immunoblot analysis. Positions of the putative mono- and di-ubiquitinated forms of wild-type Ste3p (lane *1*) are indicated by the arrows at left. The arrow at right indicates the position of a band that cross-reacts with the Ste3p-specific antibodies in these immunoblot analyses. (*B*) The effect of the *end4-1* mutation on the ubiquitination levels of the *STE3* deletion mutants. Cells of the *MATα ste3Δ end4-1* strain (NDY344) transformed by the *GAL1-STE3* plasmid pSL552 (*wt*), or by the equivalent plasmid with one of three *STE3* mutant alleles, either *STE3Δ450-468*, *STE3Δ441-468*, or *STE3Δ413-468* were grown for 2 h in galactose medium, to induce receptor expression. Further receptor synthesis was then repressed with 3% glucose and growth was continued for an additional 2 h. Extracts were prepared, treated with phosphatase, and otherwise analyzed as described above for *A*. Though the *end4* strain is temperature sensitive, the Ste3p is wholly defective for endocytosis even at permissive temperatures (Roth and Davis, 1996). Thus, in this and other experiments using the *end4-1* mutation all growth of cells is at 30°C.

in ubiquitination levels for the different receptor mutants. If, for instance, ubiquitin addition occurred at some post-surface, endosomal step, then mutations like *Δ413–468*, which block uptake, might block ubiquitination by preventing access of the receptor to downstream steps. In such an experiment (Fig. 4 *B*), essentially the same result is seen as was apparent in the $END4^+$ background (Fig. 4 *A*). While both the wild-type and *Δ450–468* receptors are ubiquitinated, the *Δ413–468* receptor is not, and the *Δ441–468* receptor shows greatly reduced levels of ubiquitination. Ste3p ubiquitination, therefore, likely occurs while receptor is surface localized, serving potentially as the initiating trigger for uptake.

Sufficiency of the Signal for Ubiquitination and Endocytosis

We have identified a domain mapping to the COOH-terminal portion of the receptor's CTD that directs both the ubiquitination and the rapid constitutive endocytosis of the receptor. In this section we test the sufficiency of this sequence to direct the ubiquitination and endocytosis of a normally long-lived constituent of the plasma membrane, the plasma membrane ATPase Pma1p. Like Ste3p, Pma1p is a polytopic plasma membrane protein with a cytoplas-

mically exposed, COOH-terminal tail. Unlike Ste3p, Pma1p is quite stable with a $t_{1/2}$ estimated at >11 h (Benito et al., 1991). By site-directed mutagenesis, an XhoI site was created at the penultimate *PMA1* codon to provide a locus for the in-frame fusion of the various *STE3* sequences to be tested. Fusions are expressed from the *GAL1* promoter, and have embedded near the NH_2-terminal–encoding end of the *PMA1* ORF, a single HA epitope tag that does not impair *PMA1* function (Harris et al., 1994). Thus, turnover of the fusion proteins may be easily assessed as follows: (*a*) PMA1-STE3 proteins are expressed via growth on galactose-containing medium, (*b*) synthesis of the construct protein is then blocked with the addition of glucose, and (*c*) the time-dependent loss is followed via immunoblotting with anti-HA mAb. This same experimental system was used previously to show that a 108-residue portion of Ste6p sufficed to direct endocytosis of a PMA1-STE6 fusion protein (Kolling and Losko, 1997).

Five different PMA1-STE3 fusion proteins were constructed, each with a different segment of the *STE3* CTD fused at the COOH terminus of *PMA1*. The parental HA-tagged Pma1p showed no evidence of turnover during the 2-h course of this experiment (Fig. 5). Attachment of the 347–398 *STE3* sequence interval was without effect; this PMA1-STE3 fusion protein shows a stability equivalent to that of the starting PMA1 construct (Fig. 5). In contrast, attachment of the 400–470 interval, encoding the COOH-terminal 71 amino acids of Ste3p, does destabilize the resulting PMA1-STE3 fusion protein (Fig. 5). This fusion protein is degraded with a $t_{1/2}$ of 40 min (Table II). Likewise, the fusion carrying the 400–449 *STE3* sequence interval also turns over (Fig. 5); a $t_{1/2}$ of 50 min is calculated for this protein (Table II). Turnover slows dramatically when the critical 414–449 interval is violated as it is for PMA1-STE3(400–440) (Fig. 5); a $t_{1/2}$ of 90 min is calculated (Table II). Finally, removal of the entire 414–449 interval, as for PMA1-STE3(400–412), effectively abolishes turnover (Fig. 5; Table II).

In addition to the five PMA1-STE3 constructs described above, four additional constructs were made with the *STE3* contribution extending various distances into the critical 414–449 interval. These constructs were subjected to analyses identical to those in Fig. 5 and the resulting calculated turnover $t_{1/2}$ is reported for each (Table II). In general, these results correlate quite well with the role of these sequences in Ste3p turnover (Fig. 3). Sequences that showed an intermediate rate of turnover in the Ste3p context also show intermediate effects when tested in the PMA1-STE3 context. In addition, we find that the minimal endocytic signal, the 414–449 *STE3* interval, suffices to promote turnover of the resulting PMA1-STE3 fusion (Table II).

Degradation of Ste3p depends on transport from the cell surface to the vacuole (Davis et al., 1993; Roth and Davis, 1996). Is the turnover of the PMA1-STE3 constructs instigated by a similar route of transport? To test involvement of vacuolar proteases in PMA1-STE3 fusion turnover, constructs with the STE3 400–449 peptide sequence interval were introduced into isogenic *PEP4*$^+$ and *pep4Δ* strains and turnover assessed. While turnover proceeds in the *PEP4*$^+$ background, in the *pep4Δ* context, turnover is completely blocked (Fig. 6, *left panel*). This is also true for the longer PMA1-STE3(400–470) fusion protein (data not shown). Thus, like wild-type Ste3p, turnover of these PMA1-STE3 fusions also depends on vacuolar proteases and therefore also likely depends on transport to the vacuole.

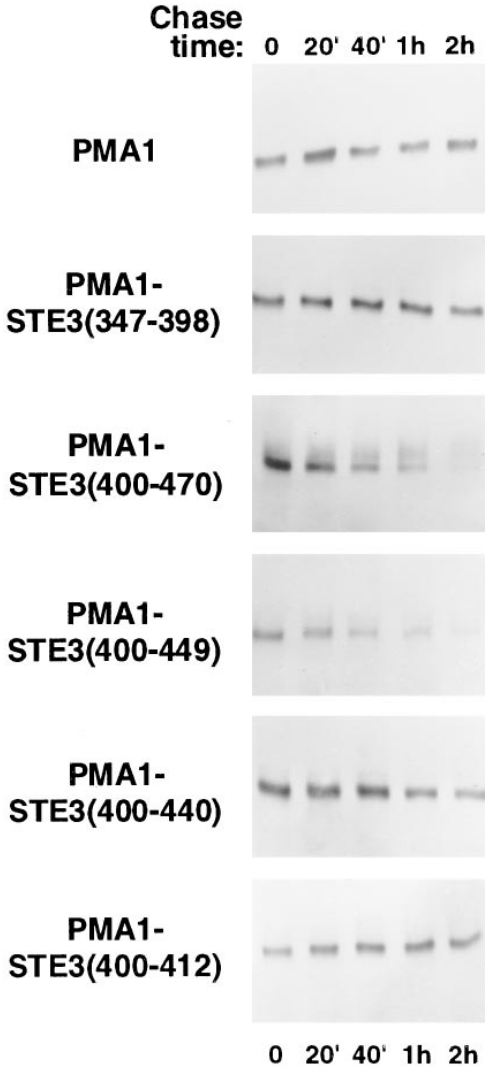

Figure 5. Stability of different PMA1-STE3 fusion proteins. Turnover analysis performed on cells of the *MAT*α strain SY1574 transformed either by a *CEN/ARS* plasmid carrying an HA epitope-tagged version of Pma1p under the control of the *GAL1* promoter (pND542) is shown in the top panel. The five panels below show the same analysis applied to cells transformed by five versions of the pND542 plasmid, having the two COOH-terminal Pma1p codons replaced by the indicated Ste3p sequence interval. For this analysis, galactose (2%) was added for 1 h, followed by the addition of glucose to 3%, and at the indicated times thereafter, culture aliquots were removed and protein extracts prepared. Extracts were subjected to SDS-PAGE, followed by immunoblot analysis using anti-HA mAb.

To test the dependence of turnover on endocytic transport, an *end4* mutant was used. The PMA1-STE3(400–449) fusion was introduced into isogenic *END4*$^+$ and *end4-1* cells. Turnover is blocked in the *end4* background (Fig. 6, *right panel*), indicating that as for Ste3p itself, turnover of the PMA1-STE3(400–449) fusion depends on its endocy-

Table II. Half-lives of PMA1-STE3 Fusion Proteins

STE3 sequences in PMA1-STE3 fusions	$t_{1/2}$ of PMA1-STE3 fusions*
none (HA-Pmalp)	>2 h
400–470	40 min
400–449	50 min
400–446	70 min
400–440	90 min
400–433	90 min
400–422	>2 h
400–412	>2 h
415–449	50 min
347–398	>2 h

*The turnover half-lives reported are the rate of loss of HA antigen at the position of full-length PMA1-STE3 fusion protein measured through AMBIS quantitative densitometry of the original films from the experiment shown in Fig. 5 and from analogous experiments.

tosis from cell surface to vacuole. Again, this is also true for the PMA1-STE3(400–470) fusion as well (data not shown).

Also apparent in the *end4* background is the presence of modified forms of the 400–449 PMA1-STE3 fusion that migrate more slowly than the mature fusion protein band (Fig. 6, species indicated by *arrowhead*). Although accentuated by *end4*, a similar modification of the PMA1-STE3(400–449) fusions was apparent both in the wild-type strain backgrounds (Fig. 5) and in the *pep4Δ* background (Fig. 6, *left panel*). Such modified species also were seen for the longer PMA1-STE3(400–470) fusion, but were not seen either for the other fusions or for the HA-tagged Pma1p alone (Fig. 7 *B*).

To test if the modification is ubiquitination, we have made use of a myc epitope–tagged ubiquitin (Ellison and Hochstrasser, 1991). Multi-copy yeast plasmids expressing either wild-type ubiquitin, the myc-tagged ubiquitin, or no ubiquitin were introduced into *end4* cells with one of three PMA1-STE3 constructs, the 400–470 fusion, the 400–449 fusion, or the long-lived 400–412 fusion. The PMA1-STE3 fusion proteins were purified from extracts of these cells via immunoprecipitation with the HA mAb. Immunoblotting of the purified fusion proteins with the HA mAb, allowed visualization of the fusion constructs and showed that overexpression of either the wild-type or epitope-tagged ubiquitin results in no obvious change in the PMA1-STE3 fusion protein electrophoretic mobility (Fig. 7 *A*). Parallel immunoblots, probed instead with the myc mAb, allowed assessment of the incorporation of the myc-tagged ubiquitin into the fusion constructs (Fig. 7 *A*). The stable 400-412 fusion, did not react with the anti-myc monoclonal (Fig. 7 *A*). In contrast, both the 400–449 and 400–470 fusions showed a clear reaction. Reaction was specific for cells coexpressing the myc epitope–tagged ubiquitin. The 400–470 fusion showed a somewhat stronger reaction than did the 400–449 fusion (Fig. 7 *A*), consistent with a greater proportion of this fusion protein being ubiquitin modified.

Using our panel of PMA1-STE3 fusions, we next tested the *STE3* sequence requirement for the ubiquitin modification. Extracts prepared from *end4* cells expressing each of the different PMA1-STE3 fusions were subjected to Western analysis with the HA mAb (Fig. 7 *B*). A prominent accumulation of modified forms is apparent for the two fusions retaining the critical 414–449 interval, i.e., the 400–449 and 400–470 fusions (Fig. 7 *B*). Smaller fusions violating the integrity of 414–449 *STE3* interval do not show this massive accumulation of modified species (Fig. 7 *B*). (The minor species migrating slightly above the major fusion protein band for each of these other fusions is not likely to represent ubiquitinated protein: the 400–412 fusion that manifests this minor species in Fig. 7 *B*, fails to react with myc mAb in Fig. 7 *A*.) Thus, just as truncation of the 414–449 interval impairs Ste3p ubiquitination, intrusion into this interval also abolishes ubiquitination of the corresponding PMA1-STE3 fusion proteins. We conclude that the 414–449 *STE3* sequence interval is the minimal signal that suffices to specify both ubiquitination and endocytosis.

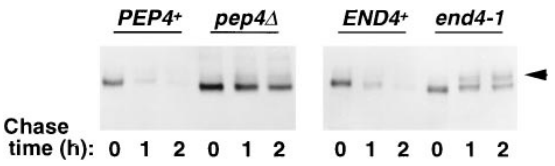

Figure 6. Effects of *pep4* and *end4* mutations on the turnover of the PMA1-STE3(400–449) fusion protein. For the experiment in the left panel, the GAL1-HA-PMA1-STE3(400–449) plasmid described for Fig. 5 was used to transform either the wild-type *MAT*α strain SY1574 (*PEP4*$^+$) or the isogenic *pep4Δ* version SY2601. For the experiment shown in the right-hand panel, the same plasmid was used to transform either the wild-type *MAT*α strain NDY334 (*END4*$^+$) or the isogenic *end4-1* version NDY335. For both experiments, after a 2-h exposure to galactose (2%), glucose was added to 3%, and at the indicated times thereafter, culture aliquots were removed and protein extracts were prepared. Extracts were subjected to SDS-PAGE, followed by immunoblot analysis using anti-HA mAb. The arrowhead to the right of the right-hand panel indicates the position of a modified form of the PMA1-STE3(400–449) fusion protein that is accentuated in extracts from the *end4* cells.

Mutational Analysis of the Endocytosis Signal

The 36-residue-long 414–449 peptide sequence comprises a ubiquitination/endocytosis signal for Ste3p. To gain insight into the nature of this sequence, we have applied alanine-scanning mutagenesis across this entire interval. Again, to avoid the potential effects of redundant signal elements within the 450–470 interval, mutations were made within the *STE3Δ450-468* context. 12 mutants in total spanning the 414–450 interval were constructed (Fig. 8). For each, three adjacent residues were substituted by three alanines. Each mutant was subjected to pulse-chase analysis identical to that previously applied to the various *STE3* deletion mutants (Figs. 1 and 2). The calculated $t_{1/2}$ are reported in Fig. 8.

Results from the alanine scanning show a good concordance with the deletion analysis (Fig. 3). While the deletion analysis indicated a requirement of the entire 414–449 interval, the 414–433 interval was found to be particularly crucial. For instance, though grossly impaired, the *Δ441–468* and *Δ434–468* receptor mutants still showed a slow

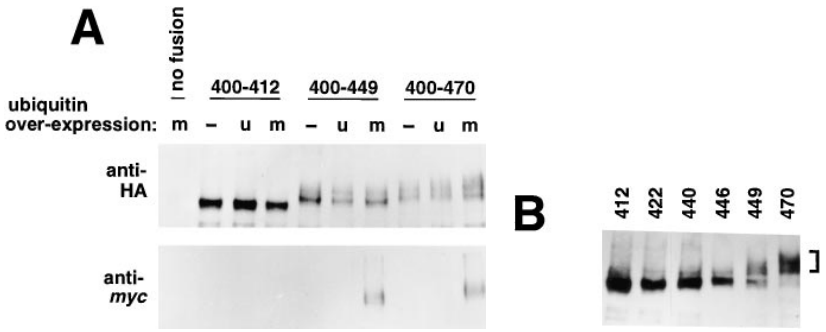

Figure 7. The STE3 signal directs ubiquitination of PMA1-STE3 fusion proteins. (*A*) Immune precipitation of PMA1-STE3 fusion proteins from *end4* cells overexpressing a myc epitope–tagged ubiquitin. Two plasmids were used to doubly transform cells of the *MAT***a** *end4-1* strain RH268-1C: (*1*) a LEU2/CEN/ARS GAL1-HA-PMA1-STE3 plasmid derived from pND542, with the STE3 contribution being either the 400–412 Ste3p interval, the 400–449 interval, or the 400–470 interval, and with (*2*) a *URA3*/2μ plasmid for *CUP1*-driven overexpression of wild-type or myc-tagged ubiquitin, either pND186 (*u*, wild-type ubiquitin), pND747 (*m*, myc-ubiquitin), pND187 (−, no ubiquitin). As an immunoprecipitation control, one cell was transformed both with the myc-ubiquitin plasmid pND747 and with the vector plasmid pRS315 (Sikorski and Hieter, 1989) in place of a PMA1-STE3–expression plasmid (*no fusion*). Transformants were subjected to a culture protocol that included growth at 30°C in media containing 100 μM $CuSO_4$ for 1 h (to induce ubiquitin expression), and then 2 h in the presence of 2% galactose (to induce PMA1-STE3 fusion protein expression), and finally 1 h in the presence of 3% glucose (to repress PMA1-STE3 expression). Extracts prepared from these cells were immunoprecipitated using the HA.11 mAb conjugated to Sepharose beads, and then subjected to SDS-PAGE followed by Western analysis. Duplicate nitrocellulose transfer membranes were developed with either the HA.11 mAb (*top panel*) or the myc mAb (*bottom panel*). (*B*) The STE3 sequence requirement for ubiquitination. Cells of the *MAT*α *end4-1* strain NDY335 were transformed by various GAL1-HA-PMA1-STE3 plasmids derived from pND542. The plasmids differ in terms of the *STE3* sequences fused at the COOH terminus. For each, the contributed *STE3* sequence extends from Ste3p residue 400 to the residue indicated above each lane. The six different transformants were subjected to a culture protocol at 30°C, which included a 1 h exposure to 2% galactose, followed by 1 h in 3% glucose. Protein extracts were prepared and analyzed as described for Fig. 5. The brackets to the right indicate the position of the more slowly migrating modified forms of the PMA1-STE3(400–449) and PMA1-STE3(400–470) fusion proteins.

rate of turnover ($t_{1/2}$ = 70 min; Fig. 3). Deletions that violated the more critical 414–433 interval (e.g., *Δ423–468* or *Δ413–468*) completely abolished turnover. Likewise for the triple alanine mutations, mutations that totally disabled endocytosis were concentrated within the crucial 414–433 interval; of the five mutants with $t_{1/2}$ of >2 h, four locate within the 414–433 interval (Fig. 8). Alanine mutations in the 434–450 interval generally showed intermediate levels of impairment (Fig. 8). The one exception to this is the replacement of the Ser-Ser-Asn 438–440 tripeptide, which appeared to fully disable endocytosis. We are presently without an explanation of how this triple alanine replacement could have a more severe phenotype than the deletion interval encompassing it.

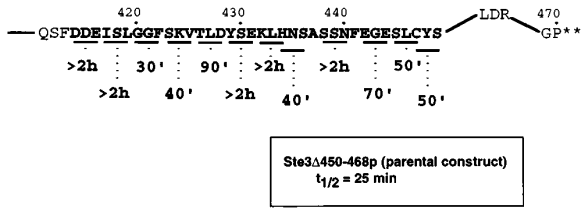

Figure 8. Effect of the triple alanine mutations on the turnover rate of Ste3Δ450-468p. The amino acid sequence of the 45 COOH-terminal residues of Ste3Δ450-468p is shown. Numbers above correspond to residue numbering of wild-type Ste3p and the minimal signal domain residues 414–449 is highlighted with bold face type. The *Δ450–468* deletion is indicated with the leucine-aspartate-arginine (LDR) tripeptide in place of the removed 19 STE3 residues. 12 mutants alleles were constructed each having three consecutive residues (*underlined*) replaced by three alanines. Strains isogenic with NDY334 except for the mutant triple alanine *STE3* allele replacement at the *STE3* locus were subjected to pulse-chase analysis identical to that of Fig. 2. The turnover $t_{1/2}$ calculated for each is indicated below.

The number of these triple alanine mutations having pronounced effects on turnover is striking (Fig. 8). Residues important for endocytosis distribute throughout the 414–450 interval. No singular sequence motif is discernible. Instead, the entire 36-residue-long sequence is required in its totality. The most prominent feature of this interval, which we later discuss, is the high proportion of acidic (glutamates and aspartates) and hydroxylated residues (serines and threonines).

Redundant Elements within the 450–470 STE3 Interval

The 414–449 sequence is the minimal ubiquitination/endocytosis signal. This, however, does not exclude the possible participation of other *STE3* sequences. A small, but reproducible effect on turnover was seen, for instance, with removal of the COOH-terminal 20 amino acids: the $t_{1/2}$ for Ste3Δ450–468p is 25 min compared with 15 min for wild-type (Fig. 2). Furthermore, like the 414–449 interval, the 450–470 interval is also rich in both acidic and hydroxylated amino acids. To test the contribution of these sequences to endocytosis, we have examined several mutations that were known to disable turnover in the *Δ450–468* receptor, within the context of the full-length receptor.

The triple alanine replacements were constructed and tested originally within the context of the *Δ450–468* deleted receptor. Two of these that had disabling effects in the *Δ450–468* receptor, were chosen and reconstructed in the full-length receptor context. The effects on the rate of receptor turnover were tested via pulse-chase analysis in both contexts (Fig. 9). In the *Δ450–468* context, both mutations severely retard endocytic turnover. Where the *Δ450–468* receptor turns over with a $t_{1/2}$ of 25 min, the same receptor with the triple alanine substitution of the Thr-Leu-Asp tripeptide at 426–428 turns over with a $t_{1/2}$ of 90 min (Fig. 9). The effect of the alanine substitution of

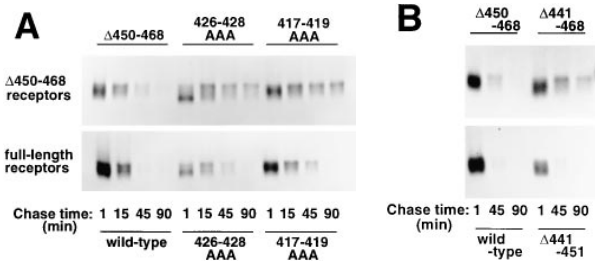

Figure 9. Comparison of effects on turnover rate of mutants constructed in the Ste3Δ450-468p receptor versus the wild-type Ste3p receptor context. Cells of strains isogenic to NDY334, except for the transplacement of the wild-type *STE3* by the indicated *STE3* mutant allele, were subjected to a pulse-chase analysis equivalent to that of Fig. 1. (*A*) Comparison of effects on turnover of two triple alanine mutations constructed either in the Ste3Δ450-468p context (*top panel*) or in the wild-type Ste3p context (*bottom panel*). The two triple alanine substitutions used for this experiment replace either the 426–428 threonine-leucine-aspartate tripeptide or the 417–419 isoleucine-serine-leucine tripeptide. (*B*) Comparison of the effects of the *Δ441–450* deletion constructed either in the Ste3Δ450-468p receptor context or in the wild-type Ste3p context.

the 417–419 tripeptide Ile-Ser-Leu is even more severe, showing a $t_{1/2}$ of >2 h (Fig. 9). In the full-length receptor context, while the two triple alanine mutations do cause some slowing of turnover, the effects are far less severe. While the wild-type receptor turns over with a $t_{1/2}$ of 12 min in this experiment, for triple alanine substitutions at 417–419 and at 426–428, turnover is slowed only to a $t_{1/2}$ of 21 and 17 min, respectively (Fig. 9). We conclude therefore that elements within the 450–470 sequence may compensate the loss of key elements in the 414–449 interval.

We have seen previously that extension of a COOH-terminal deletion from residue 450 to residue 441 severely impairs endocytic turnover (Figs. 2, 3, and 9; compare *Δ450–468* with *Δ441–468*). This implies a critical role for the 441–449 sequence. To test the importance of these sequences in an otherwise full-length receptor, we have constructed a receptor mutant in which only the 441–451 sequences are deleted. Like the two triple alanine mutants tested above, the *Δ441–451* deletion has only minor effects in the full-length receptor context (Fig. 9). Again this suggests a functional redundancy between elements in the 414–449 interval with elements in the COOH-terminal 450–470 interval. It may be that the entire 57-residue-long segment from 414 to the COOH terminus normally functions to specify Ste3p ubiquitination and endocytosis. The 414–449 interval, highlighted by our deletion analysis may correspond simply to that minimal portion still capable of promoting rapid endocytosis.

Discussion

We have characterized the sequences within the yeast **a**-factor receptor that direct its rapid, ligand-independent endocytosis. The essential sequence is striking, both in terms of its large size, minimally defined as 36 residues long, and its high density of both acidic amino acids and hydroxylated amino acids, particularly serine. Not only does this sequence specify uptake, but also ubiquitination. Receptor mutants that lack this sequence are not ubiquitinated and mutants partially deleted for this interval show a reduced level of ubiquitination that correlates well with their residual capacity for endocytosis. This sequence also is a sufficient, self-contained, transportable unit. When transplanted into the normally stable cell surface protein Pma1p, the *STE3* sequence directs both ubiquitination and endocytosis: the result being delivery of the PMA1-STE3 fusion protein to the vacuole for degradation.

Examination of the STE3 signal by visual inspection and by alanine-scanning mutagenesis reveals no obvious similarities to the short L- or Y-based peptidyl signals that mediate clathrin-dependent uptake in mammalian cells (Mellman, 1996; Schmid, 1997). Furthermore, no example of the two sequences that have been previously associated with the ligand-dependent uptake modes of the two yeast pheromone receptors are apparent (Rohrer et al., 1993; Tan et al., 1996). The large size of the STE3 ubiquitination/endocytosis signal could reflect a folding requirement to a particular three-dimensional shape for functionality. Alternatively, the functional signal could consist of an extended string or cluster of certain classes of residues. In this regard, the high proportion of both acidic and hydroxylated residues within both the 36-residue minimal signal and the more inclusive 57-residue sequence is striking. These are two of the three key sequence elements of PEST sequences, a set of sequences that act as signals for ubiquitination and consequent proteosomal turnover for various short-lived cytoplasmic and nuclear proteins. The third element of PEST sequences are prolines; there are two prolines within the COOH-terminal 57 residues of Ste3p, however, neither locate within the 414–449 interval.

PEST sequences are responsible for directing the ubiquitin-dependent proteosomal degradation of a variety of short-lived cytoplasmic and nuclear proteins (Rechsteiner and Rogers, 1996). Though PEST sequences share no primary sequence identity to one another, they do share overall character—protein sequences, 10–50-residues-long containing unusually high densities of prolines, the acidic residues glutamate and aspartate, and the hydroxylated amino acids serine and threonine. The resemblance of the STE3 signal to PEST sequences is consistent with the initiating role that ubiquitin has been proposed to play in Ste3p endocytosis (Roth and Davis, 1996). The STE3 signal may be first and foremost a signal for ubiquitination.

Recent work on two other yeast plasma membrane proteins, the **a**-factor export protein Ste6p and the uracil permease Fur4p, indicate that sequences similar to the STE3 signal likely participate in the uptake of these proteins as well (Kolling and Losko, 1997; Marchal et al., 1998). Like Ste3p, endocytosis and turnover of Ste6p and Fur4p also appear to be ubiquitin dependent (Kolling and Hollenberg, 1994; Galan et al., 1996; Loaza and Michaelis, 1998). For Ste6p, deletion of an acidic 61-residue sequence rich in serines and threonines, abolished both Ste6p ubiquitination and its rapid turnover. Though this 61-residue-long *STE6* sequence was not sufficient to direct endocytosis of a PMA1-STE6 fusion construct (equivalent in design to the PMA1-STE3 constructs used herein), a larger, more inclusive 108-residue sequence did suffice (Kolling and Losko, 1997). Mutagenic studies on Fur4p, also demon-

strate the involvement of a sequence rich in acidic and hydroxylated residues in uptake and vacuolar degradation of this permease (Marchal et al., 1998). These two sequences, together with the *STE3* sequence appear to constitute a new class of endocytosis signal—a class where the primary function of the signal may be to instigate ubiquitination.

Though resembling PEST sequences, these three ubiquitination/endocytosis signals do not score strongly as PEST sequences. This algorithm (Rogers et al., 1986) has proved to be a powerful predictor of proteins subject to rapid ubiquitin-dependent proteosomal turnover. Nonetheless, as there is little direct molecular data concerning the essential features of PEST sequences, the strictures of this algorithm are necessarily somewhat arbitrary. The algorithm examines only those sequences that are bounded by basic residues (K, R, or H), and that include at least one Pro, at least one acidic residue (D or E), and at least one hydroxylated amino acid (S or T). Of these, the strength of the resulting PEST score mostly depends on the proportion of amino acids within the interval that are either P, D, E, S, and T. The failure of the three ubiquitination/endocytosis signals to score strongly as PEST sequences reflects the paucity of proline residues within these sequences. This could indicate either that the PEST algorithm is overly stringent with regards to its proline requirement, or more interestingly, a point of functional divergence of these signals with PESTs. Although there appears to be significant overlap in the enzymatic machinery catalyzing the ubiquitination of both proteosomal substrates and cell surface proteins targeted for endocytosis (see below), the ubiquitination requirements for these two processes may be distinct. Where formation of a multi-ubiquitin chain on the substrate is generally required for proteosomal recognition (Hochstrasser, 1996), recent work on the α-factor receptor indicates that the addition of a single ubiquitin moiety suffices to direct endocytosis (Terrell et al., 1998). One possibility, therefore, is that the prolines present in the PEST sequences of proteosomal substrates play a role in specifying the construction of the multi-ubiquitin chain. In any case, as the relationship of these new endocytosis signals to PEST sequences remains uncertain, we perpetuate the term "PEST-like," coined by Marchal et al. (1998) in their description of the Fur4p signal.

The 36-residue-long STE3 signal is the minimal sequence sufficient for ubiquitination and endocytosis. PEST-like sequences in STE3, however, extend to the COOH terminus and include in addition to the 36 residues (414–449), the contiguous 21 COOH-terminal residues (450–470). We have presented evidence that this COOH-terminal sequence (450–470) may participate together in redundant fashion with the 414–449 signal. Similar redundancy may also apply within the minimal 414–449 interval. Loss of function was gradual with extension of the deletions into this interval. With extension of the deletion from residue 450 to residue 447, the $t_{1/2}$ increased from 25 to 40 min (Fig. 3, compare *Δ450–468* and *Δ447–468*). With further extension to residue 441 or to residue 434, the $t_{1/2}$ increased to 70 min (Fig. 3, *Δ441–468* and *Δ434–468*). Only deletions extending to residue 423 and residue 413 effectively abolished endocytosis (Fig. 3, *Δ423–468* and *Δ413–468*). Thus it appears that both the rate of endocytosis, and also the degree of ubiquitin modification (Fig. 3) reflects the length of the PEST-like domain remaining in each mutant. Functionality of the signal perhaps depends on its overall size and on overall density of acidic and hydroxylated residues. Larger, more negatively charged sequences may provide better substrates for ubiquitination.

Negative charge within a potential ubiquitination/endocytosis signal could be further increased through the introduction of phosphates. Such a model has been suggested both for Fur4p endocytosis (Marchal et al., 1998) and for the ligand-dependent endocytosis of Ste2p (Hicke and Riezman, 1996; Hicke et al., 1998). Addition of acidic phosphate moieties within an already acidic domain perhaps elevates a sequence through some threshold barrier of required negative charge density, allowing recognition by the E3 ubiquitination machinery. For a number of diverse proteosome substrates, phosphorylation within PEST sequences often precedes and serves to instigate subsequent ubiquitination (Hochstrasser, 1996; Rechsteiner and Rogers, 1996). This may be true for Ste3p as well, as it clearly is subject to phosphorylation (Roth and Davis, 1996).

In terms of potential ubiquitin acceptor sites, Ste3p has a total 23 cytoplasmically available lysine residues. Three map within the COOH-terminal 57-residue PEST-like sequence and of these, two within the 36-residue minimal signal. The disabling effect of the triple alanine mutation of residues 432–434 (Fig. 8) suggested the possibility that Lys432 might serve as the sole ubiquitin acceptor site within the *Δ450–468* receptor. However, this is not supported by the effects of a K432R point mutation. Within the context of the *Δ450–468* receptor, this mutation failed to block receptor ubiquitination and showed only an intermediate turnover disability ($t_{1/2}$ = 60 min; data not shown). Possibilities currently being tested are either that the ubiquitination occurs at lysines mapping outside of the PEST-like sequence and/or that multiple lysines are used redundantly.

The endocytosis signal characterized herein is also a ubiquitination signal. While decoding this signal could involve the binding of the adaptins and coat proteins, it seems more likely that initial interactions are with enzymes that catalyze ubiquitin addition. Generally for ubiquitination, although the precise biochemical or genetic requirements are incompletely understood, it is clear that the E2 and E3 classes of enzymes participate both in recognizing the substrate protein and in the subsequent ubiquitin transfer (Hochstrasser, 1996). For Ste3p ubiquitination, there are several E2 and E3 candidates. A component of the E3 complex could be the hect-domain protein Rsp5p. Though involvement in pheromone receptor endocytosis remains to be determined, *RSP5* is required for the ubiquitination and endocytic turnover of several different yeast plasma membrane proteins (Hein et al., 1995; Lucero and Lagunas, 1997). In terms of participating E2 functions, the redundant enzymes Ubc4p and Ubc5p, as well as Ubc1p are likely involved as they have been implicated in the ubiquitination and endocytosis for a variety yeast plasma membrane proteins (Kolling and Hollenberg, 1994; Egner and Kuchler, 1996; Hicke and Riezman, 1996; Roth and Davis, 1996). These E2 and E3 activities, however, can not be exclusively devoted to

plasma membrane protein turnover. Rsp5p, Ubc4p, and Ubc5p also are required for the ubiquitination and proteosomal turnover of a variety of short-lived cytoplasmic and nuclear proteins (Hochstrasser, 1996). In addition, Rsp5p recently has been implicated as a participant in the mitochondrial import process (Zolladek et al., 1997). Thus, these enzymes participate in a number of quite distinct cellular processes occurring at a number of distinct cellular sites. Specificity for membrane proteins will likely also involve the inclusion of other, presently unknown factors into these E2 and E3 complexes to direct both cellular localization and proper substrate recognition. A goal for the future, then, is to identify the specific factors that bind to and decode this new class of ubiquitination/endocytosis signal.

We thank T. Stevens for the PGK-specific antiserum and J. Haber for the HA-tagged GAL1-PMA1 plasmid.

This work was supported by a research grant from the National Science Foundation (MCB 95-06839). D.M. Sullivan was supported by a postdoctoral research fellowship from the National Institutes of Health (T32-GM08420).

Received for publication 27 February 1998 and in revised form 5 June 1998.

References

Bender, A., and G.F. Sprague, Jr. 1986. Yeast peptide pheromones, a-factor and α-factor, activate a common response mechanism in their target cells. *Cell.* 15:919–933.

Benito, B., E. Moreno, and R. Lagunas. 1991. Half-life of the plasma membrane ATPase and its activating system in resting yeast cells. *Biochim. Biophys. Acta.* 1063:265–268.

Boeke, J.D., J. Trueheart, J. Natsoulis, and G.R. Fink. 1987. 5-Fluoroorotic acid as a selective agent in yeast molecular genetics. *Methods Enzymol.* 154:164–175.

Boone, C., N.G. Davis, and G. Sprague, Jr. 1993. Mutations that alter the third cytoplasmic loop of the a-factor receptor lead to a constitutive and hypersensitive phenotype. *Proc. Natl. Acad. Sci. USA.* 90:9921–9925.

Ciechanover, A. 1994. The ubiquitin-proteosome proteolytic pathway. *Cell.* 79: 13–21.

Clark, K.L., N.G. Davis, D.K. Wiest, J.-J. Hwang-Shum, and G.F. Sprague, Jr. 1988. Response of yeast α cells to a-factor pheromone: topology of the receptor and identification of a component of the response pathway. *Cold Spring Harbor Symp. Quant. Biol.* 53:611–620.

Davis, N.G., J.L. Horecka, and G.F. Sprague, Jr. 1993. *Cis-* and *trans*-acting functions required for endocytosis of the yeast pheromone receptors. *J. Cell Biol.* 122:53–65.

Egner, R., and K. Kuchler. 1996. The yeast multidrug transporter Pdr5 of the plasma membrane is ubiquitinated prior to endocytosis and degradation in the vacuole. *FEBS (Fed. Eur. Biochem. Soc.) Lett.* 378:177–181.

Ellison, M.J., and M. Hochstrasser. 1991. Epitope-tagged ubiquitin: a new probe for analyzing ubiquitin function. *J. Biol. Chem.* 266:21150–21157.

Galan, J., and R. Haguenauer-Tsapis. 1997. Ubiquitin Lys63 is involved in ubiquitination and endocytosis of a yeast plasma membrane protein. *EMBO (Eur. Mol. Biochem. Organ.) J.* 16:5847–5854.

Galan, J.M., V. Moreau, B. Andre, C. Volland, and R. Haguenauer-Tsapis. 1996. Ubiquitination mediated by the Npi1p/Rsp5p ubiquitin-protein ligase is required for endocytosis of the yeast uracil permease. *J. Biol. Chem.* 271: 10946–10952.

Givans, S.A., and G.F. Sprague, Jr. 1997. The ankyrin repeat-containing protein Akr1p is required for the endocytosis of yeast pheromone receptors. *Mol. Biol. Cell.* 8:1317–1327.

Gowers, R., P. van Kerkhof, A.L. Schwartz, and G.J. Strous. 1997. Linkage of the ubiquitin-conjugating system and the endocytic pathway in ligand-induced internalization of the growth hormone receptor. *EMBO (Eur. Mol. Biochem. Organ.) J.* 16:4851–4858.

Hagen, D.C., G. McCaffrey, and G.F. Sprague, Jr. 1986. Evidence that the yeast *STE3* gene encodes a receptor for peptide pheromone a-factor. *Proc. Natl. Acad. Sci. USA.* 83:1418–1422.

Harris, S.L., S. Na, X. Zhu, D. Seto-Young, D. Perlin, J.H. Teem, and J.E. Haber. 1994. Dominant lethal mutations in the plasma membrane H^1-ATPase gene of *Saccharomyces cerevisiae*. *Proc. Natl. Acad. Sci. USA.* 91:10531–10535.

Hein, C., J.-Y. Springael, C. Volland, R. Haguenauer-Tsapis, and B. Andre. 1995. *NPI1*, an essential yeast gene involved in induced degradation of Gap1 and Fur4 permeases, encodes the Rsp5 ubiquitin-protein ligase. *Mol. Microbiol.* 18:77–87.

Hicke, L., and H. Riezman. 1996. Ubiquitination of a yeast plasma membrane receptor signals its ligand-stimulated endocytosis. *Cell.* 84:277–287.

Hicke, L., B. Zanolari, and H. Riezman. 1998. Cytoplasmic tail phosphorylation of the α-factor receptor is required for ubiquitination and internalization. *J. Cell Biol.* 141:359–371.

Hochstrasser, M. 1996. Ubiquitin-dependent protein degradation. *Annu. Rev. Genet.* 30:405–439.

Kolling, R., and C.P. Hollenberg. 1994. The ABC-transporter Ste6 accumulates in the plasma membrane in a ubiquitinated form in endocytosis mutants. *EMBO (Eur. Mol. Biochem. Organ.) J.* 13:3261–3271.

Kolling, R., and S. Losko. 1997. The linker region of the ABC-transporter Ste6 mediates ubiquitination and fast turnover of the protein. *EMBO (Eur. Mol. Biochem. Organ.) J.* 16:2251–2261.

Kunkel, T.A., J.D. Roberts, and R.A. Zakour. 1987. Rapid and efficient site-specific mutagenesis without phenotypic selection. *Methods Enzymol.* 154: 367–382.

Loaza, D., and S. Michaelis. 1998. Role of the ubiquitin-proteosome system in the vacuolar degradation of Ste6p, the a-factor transporter in *Saccharomyces cerevisiae. Mol. Cell. Biol.* 18:779–789.

Lucero, P., and R. Lagunas. 1997. Catabolite inactivation of the yeast maltose transporter requires ubiquitin-ligase npi1/rsp5 and ubiquitin-hydrolase npi2/doa4. *FEMS (Fed. Eur. Microbiol. Soc.) Microbiol. Lett.* 147:273–277.

Marchal, C., R. Haguenauer-Tsapis, and D. Urban-Grimal. 1998. A PEST-like sequence mediates phosphorylation and efficient ubiquitination of yeast uracil permease. *Mol. Cell. Biol.* 18:314–321.

Mellman, I. 1996. Endocytosis and molecular sorting. *Annu. Rev. Cell Dev. Biol.* 12:575–625.

Payne, G.S., D. Baker, E. van Tuinen, and R. Schekman. 1988. Protein transport to the vacuole and receptor-mediated endocytosis by clathrin heavy chain-deficient yeast. *J. Cell Biol.* 106:1453–1461.

Raths, S., J. Rohrer, F. Crausaz, and H. Riezman. 1993. *end3* and *end4*: Two mutants defective in receptor-mediated and fluid-phase endocytosis in *Saccharomyces cerevisiae*. *J. Cell Biol.* 120:55–65.

Rechsteiner, M., and S.W. Rogers. 1996. PEST sequences and regulation by proteolysis. *Trends Biochem. Sci.* 21:267–271.

Riezman, H., A. Munn, M.I. Geli, and L. Hicke. 1996. Actin-, myosin- and ubiquitin-dependent endocytosis. *Experientia (Basel).* 52:1033–1041.

Rogers, S., R. Wells, and M. Rechsteiner. 1986. Amino acid sequences common to rapidly degraded proteins: the PEST hypothesis. *Science.* 234:364–368.

Rohrer, J., H. Benedetti, B. Zanolari, and H. Riezman. 1993. Identification of a novel sequence mediating regulated endocytosis of the G-protein-coupled α-pheromone receptor in yeast. *Mol. Biol. Cell.* 4:511–521.

Rose, M.D., P. Novick, J.H. Thomas, D. Botstein, and G.R. Fink. 1987. A *Saccharomyces cerevisiae* genomic plasmid bank based on a centromere-containing shuttle vector. *Gene.* 60:237–243.

Roth, A.F., and N.G. Davis. 1996. Ubiquitination of the yeast a-factor receptor. *J. Cell Biol.* 134:661–674.

Schmid, S.L. 1997. Clathrin-coated vesicle formation and protein sorting: an integrated process. *Annu. Rev. Biochem.* 66:511–548.

Sikorski, R.S., and P. Hieter. 1989. A system of shuttle vectors and yeast host strains designed for efficient manipulation of DNA in *Saccharomyces cerevisiae. Genetics.* 122:19–27.

Strous, G.J., P. van Kerkhof, R. Govers, A. Ciechanover, and A.L. Schwartz. 1996. The ubiquitin conjugation system is required for ligand-induced endocytosis and degradation of the growth hormone receptor. *EMBO (Eur. Mol. Biochem. Organ.) J.* 15:3806–3812.

Tan, P.K., N.G. Davis, G.F. Sprague, Jr., and G.S. Payne. 1993. Clathrin facilitates the internalization of seven transmembrane segment receptors for mating pheromones in yeast. *J. Cell Biol.* 123:1707–1716.

Tan, P.K., J.P. Howard, and G.S. Payne. 1996. The sequence NPFXD defines a new class of endocytosis signal in *Saccharomyces cerevisiae. J. Cell Biol.* 135: 1789–1800.

Terrell, J., S. Shih, R. Dunn, and L. Hicke. 1998. A function for monoubiquitination in the internalization of a G protein-coupled receptor. *Mol. Cell.* 1:193–202.

Zolladek, T., A. Tobiasz, G. Vaduva, M. Boguta, N.C. Martin, and A.K. Hopper. 1997. *MDP1*, a *Saccharomyces cerevisiae* gene involved in mitochondrial/cytoplasmic protein distribution, is identical to the ubiquitin-protein ligase gene *RSP5. Genetics.* 145:595–603.